

Diagnostics of Transient Sprays by Means of Laser Sheet Techniques

T.Kamimoto

*Department of Mechanical Engineering
Tokyo Institute of Technology
Ookayama 2-12-1, Meguro-ku, Tokyo 152
Japan*

ABSTRACT

This article summarizes recent work that has been performed by the author's group at Tokyo Institute of Technology in the field of 2-D imaging diagnostics of diesel fuel sprays. The work was concentrated on enhancing the capabilities of quantitative measurement by some of the techniques in 2-D imaging diagnostics. Experiments were conducted applying these techniques to non-evaporating, evaporating, and combusting sprays achieved in the optically accessible chamber of a rapid compression machine. Selected 2-D contour mappings of droplet size, fuel vapor concentration and soot concentration are presented. It is shown that soot formation is closely related to the fuel vapor concentration distribution in the spray.

INTRODUCTION

The use of laser sheet as the incident light to particles or molecules in the spray permits to obtain instantaneous 2-D distributions of droplet size, fuel vapor concentration and soot concentration. All of these 2-D images are expected to give significant insight into formation and extinction processes of NO_x and particulates in the engine cylinder. They also seem valuable in validating mathematical models under development. This paper summarizes recent work that has been performed by the author's group at Tokyo Institute of Technology in the field of 2-D imaging diagnostics of diesel sprays. Experiments were carried out by using an optical system and a rapid compression machine in which non-evaporating, evaporating and combusting sprays were achieved.

Droplet sizing may seem useless in diesel engine research as the fuel injected into the engine cylinder evaporates rapidly under normal operating condition. But droplet sizing is still important because atomization is one of the primary spray characteristics which governs evaporation under various conditions such as cold starting condition. A new technique, "Fluorescence-scattering emission imaging technique", was developed by the author's group which is different from the point-by-point measurement techniques such as PDA and Fraunhofer diffraction technique and can

give instantaneous 2-D droplet size distribution in non-evaporating sprays. The principle of this technique and its application to non-evaporating sprays will be given.

The exciplex-based fluorescence technique has been widely used for visualizing liquid and vapor phase in evaporating sprays. Intensive work has been performed to make this technique to be applied to the quantitative measurement of fuel vapor concentration in engine-like environment. The result of calibration, i.e. the relationship between fluorescence intensity and vapor concentration will be shown with vapor temperature as a parameter. In addition to this, a new technique called "Silicone oil particle scattering technique" developed also at the author's laboratory will be outlined, and some of the 2-D contour mappings of the equivalence ratio in an evaporating spray will be presented.

The elastic scattering technique developed for 2-D soot imaging was assessed by a comparison with the laser induced incandescence technique, and was applied to combusting sprays. Furthermore, an image processing technique to obtain 2-D velocity vector distribution from a pair of elastic scattering images taken at a short time interval was developed. The results of 2-D mappings of velocity vector and soot concentration are compared with that of fuel vapor concentration, and soot formation and oxidation processes are discussed.

EXPERIMENTAL SETUP AND OPTICAL SYSTEM

In all experiments conducted in this study, a rapid compression machine was used which has a combustion chamber with a bore of 196 mm, a thickness of 40 mm at TDC, and a compression ratio of 14.7. Fuel was injected into the chamber using an electro-hydraulic control unit injector at constant injection pressures ranging from 30 MPa to 135 MPa. A single hole nozzle with 0.15 mm or 0.2 mm diameter and a length to diameter ratio of 4 was used. Fig. 1 shows the rapid compression machine equipped with the unit injector and the optical setup used commonly in experiments. In 2-D drop size measurement, a non-evaporating spray was achieved in the combustion chamber filled with nitrogen having a room temperature and a high pressure. In 2-D quantitative measurement of fuel vapor concentration in a transient

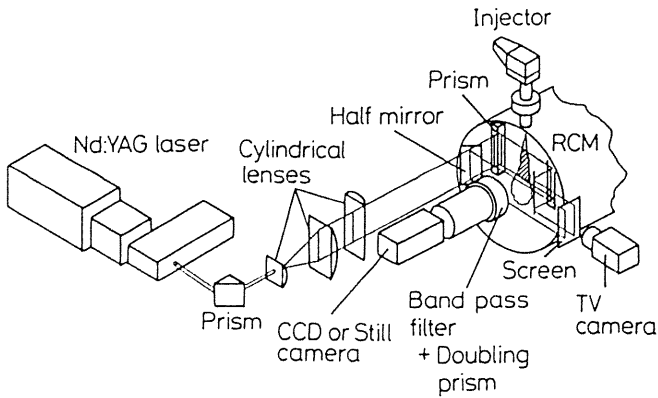


Fig. 1 Optical setup and rapid compression machine

evaporating spray, fuel was injected into a rapidly compressed nitrogen with a high temperature and a high pressure. In experiment of 2-D soot imaging, a transient combusting spray was formed in a rapidly compressed air at a high temperature and a high pressure.

The laser beam of a Nd-YAG laser (Quanta-Ray DCR-11, 275 mJ/pulse at 1064 nm) was expanded vertically and collimated by two cylindrical lenses to form a laser sheet having an approximately 0.2 ~ 0.3 mm thickness on the spray axis and 40 mm height. The laser sheet which passed through the optical window of the combustion chamber was reflected by a prism located inside the combustion chamber and propagated through the mid-plane of a spray. The images of fluorescence and scattering from fine particles were taken by a high-speed gated image intensifier (Hamamatsu Photonics C2925) through an optical filter selected for each experiment. The image frozen on the phosphor of the intensifier was taken by a CCD camera (NEC, TI-22AII: 378 x 485 pixels) via a relay lens, and was digitized by an image processor (ADS IP4: 8bit, 512 x 512 pixels). The image data was processed by a

personal computer (HP series 9000 model 300). A doubling prism and two suitable filters were placed in front of the object lens of the image intensifier to take two images simultaneously. The optical characteristics of filters as well as the laser power and wavelength employed in each experiment are summarized in Table 1.

MEASUREMENT OF DROP SIZES IN TRANSIENT SPRAYS

Measurement Principle

The 2-D distribution of the local Sauter mean diameter of droplets in a non-evaporating spray was measured by a new technique which is based on an analysis of laser induced fluorescence and elastic scattering images taken simultaneously.[1] A small fraction of a dopant is dissolved in a base fuel, and the dopant can be excited by an appropriate ultraviolet light to form a fluorescence emission. When a laser sheet light irradiates a plane including the spray axis, the fluorescence and scattering lights are emitted simultaneously from the droplets, and both emissions are imaged from a direction perpendicular to the plane of the laser sheet light. Since the fluorescence intensity is proportional to droplets cubed if the droplet diameter is smaller than 80 μm [2], the fluorescence intensity, $i_f(r, z)$, can be written in r, z, θ coordinates system as follows.

$$i_f(r, z) = I_0 \cdot e^{-kx} \cdot C_1 \cdot \int_0^{\infty} D^3 \cdot \frac{dn}{dD} \cdot dD \quad (1)$$

where I_0 is the incident light intensity which will attenuate with kx obeying the Beer's law, x is the distance from the incident side boundary, and k is the attenuation coefficient. D is particle diameter, dn is the number density of particles

Table 1 Object to be measured, fuel composition, phenomena focused and optical characteristics of laser and optical filter

Object	Subject measured	Fuel composition	Laser pulse, wavelength, power, duration	Phenomena focused	Optical filter central wavelength and FWHM
Non-evaporating spray	Drop size	0-solvent* (99 %) ** + TMPD (1 %)	355 nm 60 mJ, 8 ns	Elastic scattering	355 nm (14 nm)
				LIF (TMPD)	398 nm (20 nm)
Evaporating spray	Fuel vapor concentration	0-solvent (94.5 %) + Naphthalene (5.0 %) + TMPD (0.5 %)	355 nm 60 mJ, 8 ns	LIF (TMPD)	398 nm (20 nm)
				Elastic scattering	No filters
Combusting spray	Soot concentration	0-solvent or 0-solvent (75 %) + Ethanol (20 %) + n-octanol (5 %)	1064 nm + 532 nm 260 mJ, 8 ns	Laser Induced Incandescence	400 nm (30 nm)
			532 nm, 135 mJ	Elastic scattering	532 nm (4 nm)

* 0-solvent; $C_{12}H_{26}$: 22 %, $C_{13}H_{28}$: 54 %, $C_{14}H_{30}$: 24 %

** by mass

with diameter between D and $D + dD$, and C_1 is a constant value which includes the absorption coefficient, quantum yield and detecting system characteristics. On the other hand, the Mie's scattering intensity $i_s(r, z)$ is proportional to diameter squared as given by Eq.(2)

$$i_s(r, z) = I_0 e^{-kx} C_2 \int_0^{\infty} Q_{sca}(\alpha, \theta, \Delta\theta) \cdot D^2 \cdot \frac{dn}{dD} dD \quad (2)$$

where C_2 is a constant relating to the detecting system characteristics. The Mie's scattering coefficient, $Q_{sca}(\alpha, \theta, \Delta\theta)$, is a function of particle parameter, $\alpha = \pi D/\lambda$, where λ is the incident light wavelength, θ , the scattering angle, and $\Delta\theta$, the detection angle. When assuming a particle size distribution for the particles, we can define an average scattering coefficient, $Q_{sca}(\alpha_{32}, \theta, \Delta\theta)$. Where $\alpha_{32} = \pi D_{32}(r, z)/\lambda$, and $D_{32}(r, z)$ is the local Sauter mean diameter. Now we can determine local Sauter mean diameter $D_{32}(r, z)$ from the measured values of fluorescence intensity $i_f(r, z)$ and scattering intensity $i_s(r, z)$ using the following equation.

$$D_{32}(r, z) = \frac{\int_0^{\infty} D^3 \cdot \frac{dn}{dD} dD}{\int_0^{\infty} D^2 \cdot \frac{dn}{dD} dD} = \frac{Q_{sca}(\alpha_{32}, \theta, \Delta\theta)}{C} \cdot \frac{i_f(r, z)}{i_s(r, z)} \quad (3)$$

An iterative calculation is needed to get the final value of $D_{32}(r, z)$ because $Q_{sca}(\alpha_{32}, \theta, \Delta\theta)$ is a function of $D_{32}(r, z)$.

Experimental

In order to obtain the fluorescence emission from particles in fuel sprays, 1% by weight of NNN'N'-tetramethyl-p-phenylene diamine (TMPD) was dissolved in the base fuel, 0-solvent ($C_{12}H_{26}$: 22%, $C_{13}H_{28}$: 54%, $C_{14}H_{30}$: 24%). The fuel was injected into a nitrogen atmosphere with a density of 17 kg/m^3 and a temperature of 293 K. The spray was irradiated by the single pulsed laser sheet light with a wavelength of 355 nm at various times after the start of injection.

The laser induced fluorescence emission was transmitted through a band pass filter with a central wavelength of 398 nm and a FWHM of 20 nm. The scattering emission was transmitted through a band pass filter with a center wavelength of 355 nm and a FWHM of 13.6 nm. Since the intensities of the fluorescence and scattering emissions are different, a neutral density filter was used to attenuate the scattering emission intensity. The spectral characteristics of the filters as well as that of TMPD are shown in Fig. 2.

The laser sheet with a height of 40 mm was shifted to three positions; 0~40, 30~70, and 60~100 mm from the nozzle orifice to cover the whole domain of the spray penetration. Since the signal intensity becomes weaker with the distance, the gain of the image intensifier was adjusted depending on the laser sheet position. Fig. 3 shows a typical pair of fluorescence and scattering emission images.

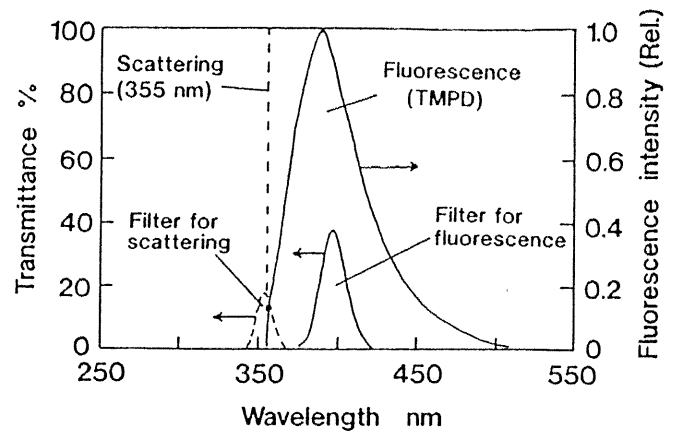


Fig. 2 Fluorescence spectra of TMPD and transmissivities of the filters used[1]

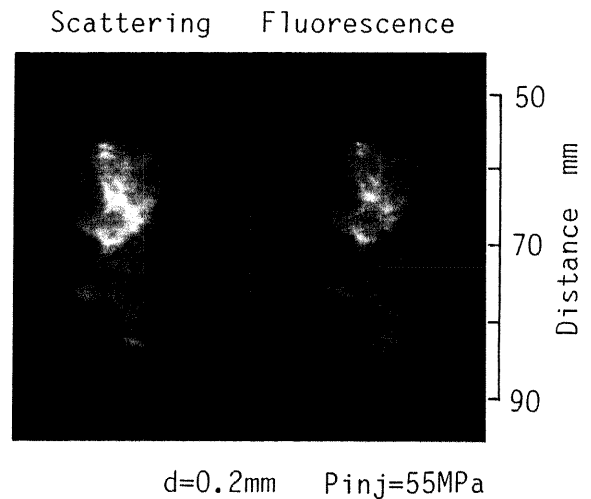


Fig. 3 A typical pair of fluorescence and elastic scattering emission images

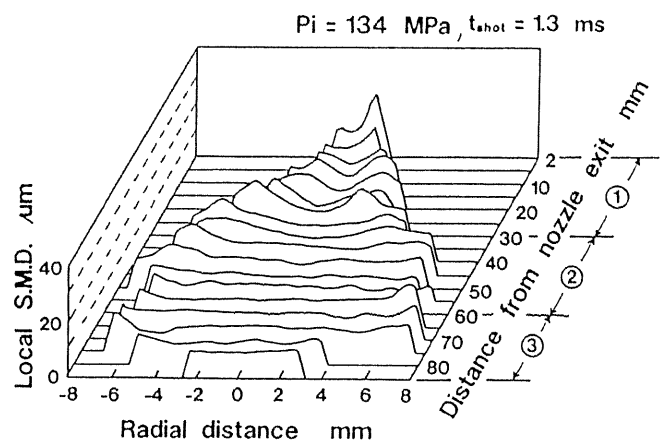


Fig. 4 2-D distribution of $D_{32}(r, z)$ at $P_i = 134 \text{ MPa}$ [1]

Results and Discussions

Fig. 4 shows the 2-D distribution of local Sauter mean diameter, $D_{32}(r,z)$, for a fuel injection pressure of 134 MPa. $D_{32}(r,z)$ along the spray axis shows a gradual decrease with distance from the nozzle, and after exhibiting a minimum value at around 20 mm, $D_{32}(r,z)$ increases again toward the spray tip. This tendency is common to other two cases with different injection pressures, and shows a qualitative agreement with the computational results obtained by Reitz et al.[3]. $D_{32}(r,z)$ distribution in radial direction shows larger droplet size in the spray periphery. This result agrees well with that of Gülder et al.[4] who used the Fraunhofer diffraction method for the particle size measurement.

QUANTITATIVE MEASUREMENT OF FUEL VAPOR CONCENTRATION IN TRANSIENT EVAPORATING SPRAYS

Exciplex-Based Fluorescence Technique[5]

Principle and calibration. Exciplex-based fluorescence technique developed by Melton et al.[6] was used to visualize the liquid and vapor phase in an evaporating spray. If the concentration fraction of TMPD and naphthalene used for the fluorescence molecules are selected appropriately, the fluorescence emission from TMPD* may be a hundred times that from the exciplex of (naphthalene / TMPD)* in the vapor phase. Accordingly the fluorescence emission from TMPD* was taken note for the quantitative measurement of fuel vapor concentration in an evaporating spray.

When being exposed to a high temperature and high pressure engine-like environment, TMPD may undergo thermal decomposition during several milliseconds of observation. To give an answer to this question, an experiment was conducted using a rapid compression expansion machine having a bore of 50 mm and a compression ratio of 5. TMPD was dissolved in decane at a ratio of 8 gram TMPD per a liter of decane, and the TMPD doped decane was injected quickly into the cylinder charged with nitrogen of 0.1 MPa and 423 K at BDC. After the evaporated TMPD and decane vapor being uniformly distributed in nitrogen, the mixture was compressed in 20 ms. The piston was kept stationary at TDC for about 10 ms, and during this period the laser beam irradiated the compressed mixture to generate fluorescence emission. When one shot experiment was accomplished, the mixture used was discharged and then the chamber was charged with new TMPD dissolved fuel for the next run. The result showed that the fluorescence intensity did not change during 10 ms at a condition of 680 ~ 740 K and 1.75 ~ 1.95 MPa.

Secondly the relationship between TMPD vapor concentration and fluorescence intensity under engine-like environment was calibrated using the rapid compression-expansion machine. In the experiment, a square piston installed in an optically accessible square chamber which has a cross section of 60 mm x 60 mm was actuated by the machine. A TMPD solution composed of 1 % TMPD and 99 % of decane by weight was injected into the chamber by a microsyringe when the piston is positioned at BDC, and was

mixed with nitrogen at a temperature of 423 K. After the solution completes evaporation and mixing with nitrogen, the mixture was compressed rapidly in 20 ms and was maintained at an almost constant condition during 10 ms at TDC position. At 3 ms after the end of compression, the laser beam with a wavelength of 355 nm, a power output of 60 mJ, and a pulse duration of 8 ns was shot into the chamber through the side quartz window. The fluorescence emission was imaged from the direction right to the incident beam through a quartz window head. At the same time, the intensity of the laser beam was detected at each shot to correct the effect of the shot-by-shot fluctuation of the laser power.

Fig. 5 shows an example of the relationship between TMPD vapor concentration and the fluorescence intensity at three different temperatures. The figure indicates that fluorescence intensity is proportional to the TMPD vapor concentration at a constant temperature in the range of 550 K to 800 K. It also shows a lower sensitivity of the fluorescence intensity to TMPD concentration at high temperatures. This demands a knowledge of the local vapor temperature for the quantitative measurement of the vapor concentration. Since the adiabatic equilibrium condition holds reasonably for the vapor-gas mixture in evaporating sprays, the mixture temperature can be calculated by an energy equation as a function of the vapor concentration and the surrounding gas condition. Consequently, both the temperature and the concentration can be determined simultaneously by an iterative calculation using the calibration relationship and the energy equation.

Experimental. TMPD and naphthalene were dissolved by 0.5 % and 1 % respectively in a normal paraffin base fuel. The spectral characteristics of filters used for detecting the TMPD and the exciplex-based fluorescence are listed in Table 1.

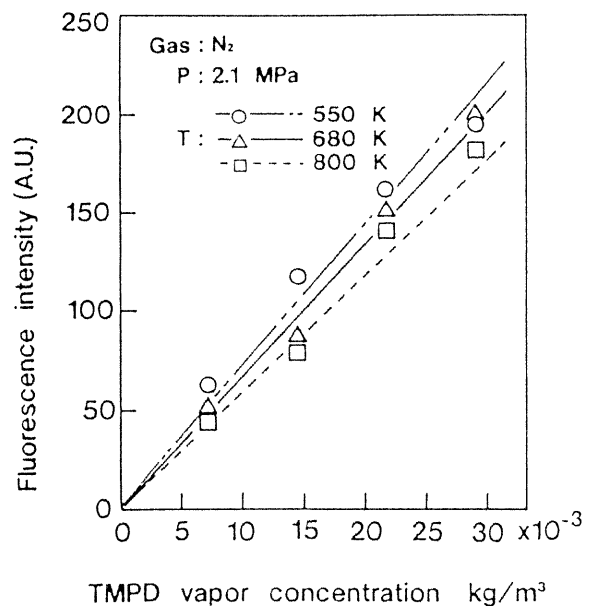


Fig. 5 Relationship between TMPD vapor concentration and fluorescence intensity with vapor temperature as a parameter[5]

The fuel was injected into a rapidly compressed nitrogen at a temperature of 630 K and a density of 14 Kg/m³. The intensity distribution of the laser sheet was measured prior to the experiment for a correction of the fluorescence image.

Results and Discussions. Fig. 6 provides contour mappings of the fuel vapor concentration and the fuel vapor temperature distribution of a transient evaporating spray after the end of injection. To assess the accuracy of the measured fuel vapor concentration distribution, the mass of the fuel vapor was integrated over the entire image of the fuel vapor concentration on the assumption of the axisymmetry of the spray, and the integrated fuel mass was compared with the total amount of injected fuel. It was shown that the normalized fuel mass lies on a reasonable level between 0.8 ~ 0.9 after the end of injection. The reason for the normalized fuel mass being less than 1.0 could be attributed to the undetection of the leanest mixture in the edge of the spray.

Silicone Oil Particle Scattering Technique[7]

Principle and calibration. A mass fraction of 1 % of silicone oil was dissolved in the base fuel. When the silicone-dissolved fuel is injected into a nitrogen at a temperature of 640 K, the volatile base fuel in the droplets will vaporize rapidly, leaving behind small droplets of the nonvolatile

silicone oil suspended in the vapor-gas mixture. The diameter of silicone oil droplet can be calculated as 4.2 μm if the initial diameter of fuel droplet is assumed 20 μm. The silicone oil droplet of this size was estimated to follow fully turbulence motion at a frequency below 2 KHz.

The silicone oil droplets illuminated by the laser sheet emit the elastic scattering, and the intensity will represent in good approximation the fuel vapor concentration in an evaporating spray provided that the evaporation of base fuel is complete and the size of silicone oil droplet is uniform. The fuel vapor concentration can be expressed by the following equation.

$$C_f = \kappa \frac{2 I_{CCD} D_{32} \rho}{3 Q_{sca} X} \quad (4)$$

where κ is a constant ; I_{CCD} , detected intensity of scattering emission; D_{32} , diameter of silicone oil droplet; ρ , density of silicone oil; Q_{sca} , scattering coefficient of silicone oil droplet; X , mass fraction of dissolved silicone oil. The value κ was determined by a calibration experiment using a suspension of glass beads in ethanol. In spray experiments, the diameter of silicone oil droplet, D_{32} , was calculated by an empirical equation which formulates the fuel droplet diameter in a diesel spray as a function of orifice diameter, injection pressure and surrounding gas density.

Experimental. The silicone dissolved fuel was injected into nitrogen at a temperature of 630 K and a density of 14 Kg/m³. The laser sheet was divided into two paths by a beam-splitter (transmittance: 45 %, reflectance: 55 %) placed in front of the combustion chamber. The laser sheet reflected by the beam-splitter was projected on a screen and the image was detected by a TV camera (Hamamatsu C2741-7) to measure the intensity distribution of the incident laser sheet.

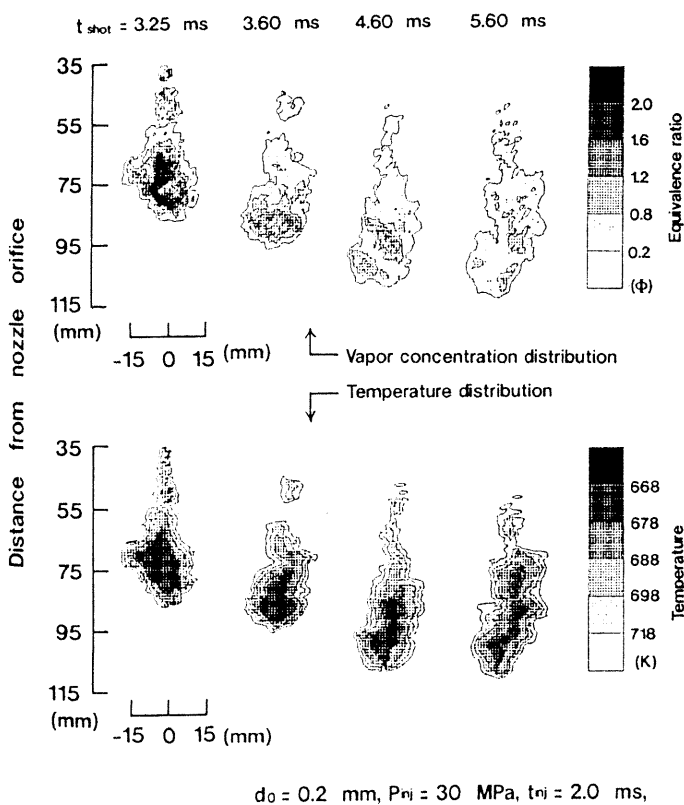


Fig. 6 Contour mappings of equivalence ratio and fuel vapor temperature distribution in an evaporating spray

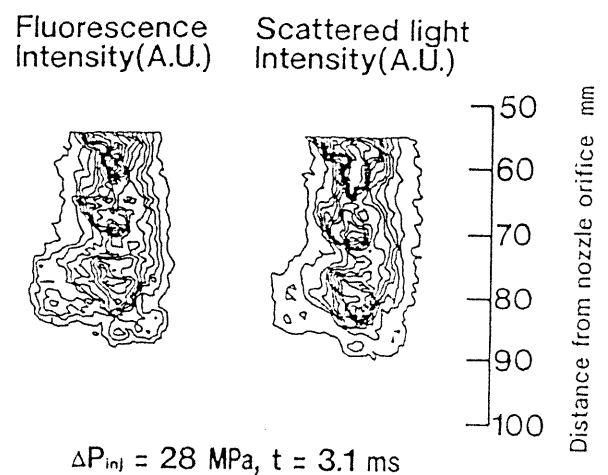


Fig. 7 Cross sectional patterns of TMPD fluorescence intensity and silicone oil particle scattering intensity in an evaporating spray

The first experiment we have done for the assessment of the proposed technique was a qualitative comparison between the scattering and the exciplex-based fluorescence image of a fuel vapor concentration distribution in an evaporating spray. In this comparison, the effect of fuel vapor temperature on TMPD fluorescence emission was not taken into account, but both images showed relatively good agreement as shown in Fig. 7. The cross correlation coefficients calculated for several pairs of images were above 0.93, showing a significant similarity between the silicone oil droplet scattering image and the fluorescence emission image.

Results and discussions. Fig. 8 shows the cross-sectional distributions of equivalence ratio in an evaporating spray at an injection pressure of 140 MPa. The equivalence ratio was calculated from the vapor concentration, C_p , on the assumption that the density of the entrained gas is uniform throughout the evaporating spray. This assumption tends to make the equivalence ratio in a fuel rich region to be higher than the real value. The images on the top row of the figure are the equivalence ratio distributions taken at 1.0 ms after the start of injection for three different runs respectively, and show run-by-run variation in equivalence ratio distribution. The images on the bottom are those taken at 1.4 ms after the start of injection.

The fuel vapor-gas mixtures having spatial scales with several millimeters are distributed unevenly, and fuel rich

mixtures are observed to travel downward along the spray axis showing wavy patterns. It is interesting to note that puffs of fuel rich mixtures are distributed discontinuously in flow direction at an interval of several to ten millimeters. Also interesting are the existence of isolated small mixture islands in the surrounding atmosphere and of entrained gas pockets in the vapor phase. As compared to the equivalence ratios in the central region, the equivalence ratio in the peripheral region are extremely low. In the spray head region, the equivalence ratio decreases steeply toward the spray tip.

One of the major advantages of the silicone oil particle scattering technique is the strong emission intensity sufficient to be detected with conventional films. This made it possible to take high speed photographs of 2-D images of fuel vapor concentration distribution of an evaporating spray using a laser sheet formed with a copper vapor laser (NEC GLD 7010, 1 mJ/pulse, 20 ~ 40 ns in Pulse duration). The continuously taken photographs disclosed a fact that puffs of fuel vapor with high concentrations flow downward periodically.

In the case of combusting spray, when ignition starts about 1.0 ms after the start of injection, the region from 50 mm to the spray tip expands instantaneously due to the exothermic reaction. The condition of fuel vapor-air mixing when the ignition starts is presented by the images taken at 1.0 ms in Fig. 8. The central part of the spray between 60 to 70 mm from the nozzle orifice includes mixtures with around stoichiometry. But in the region from 70 mm to the spray tip,

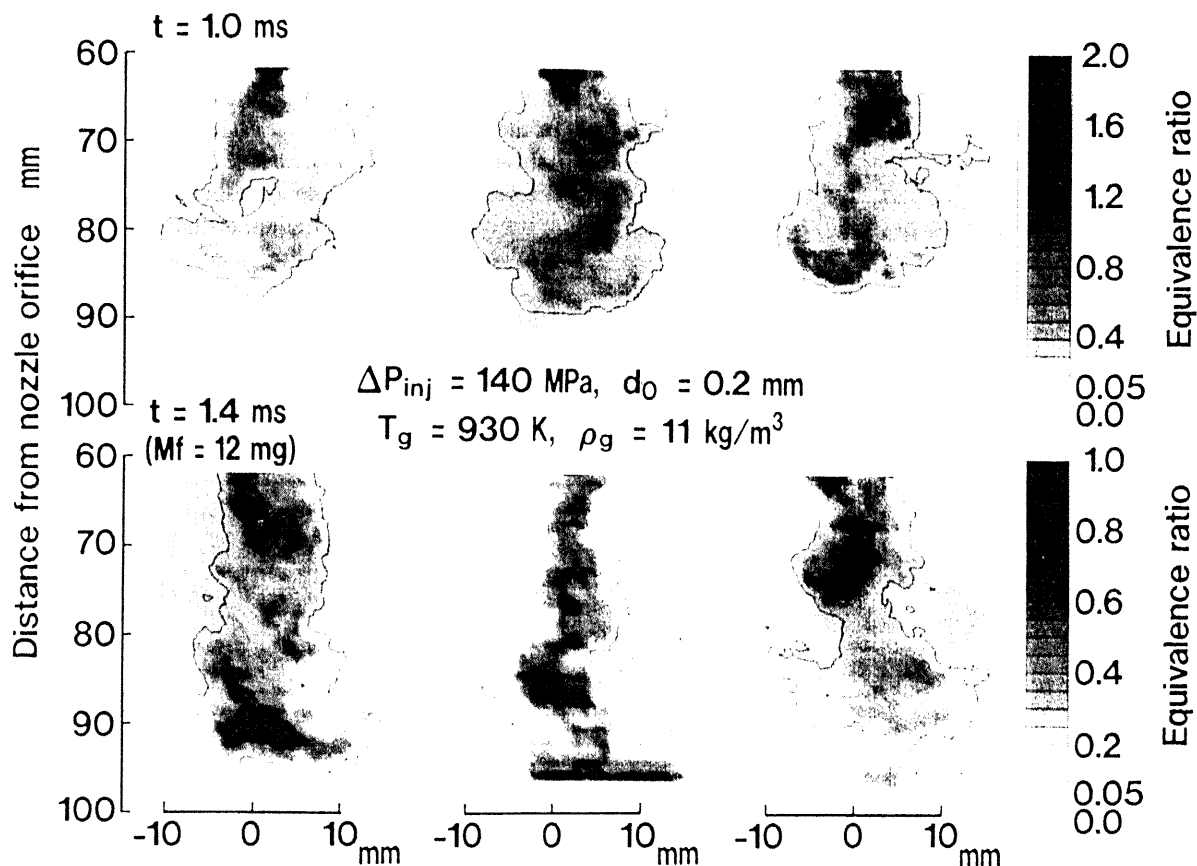


Fig. 8 Cross sectional distribution of equivalence ratio in an evaporating spray[7]

mixtures with equivalence ratio lower than stoichiometry are prevailing. It is hard to point the location where the ignition starts because ignition delay depends not only the equivalence ratio but also the temperature of mixtures as well as the lapse of time for each mixture element.

Soot cloud starts to appear in the middle of the flame at around 1.5 ms after the start of injection, in the latter half of the initial combustion phase or the early stage of diffusion combustion phase. The equivalence ratio images at 1.4 ms shown on the bottom in Fig. 8 represent the condition in the spray at this moment. Mixtures with around stoichiometric equivalence ratio are unevenly distributed in the central region surrounded by lean mixtures. The soot cloud which emerges first in the laser shadow pictures seems to appear in those relatively rich mixtures.

MEASUREMENT OF SOOT CONCENTRATION IN TRANSIENT COMBUSTING SPRAYS

LII and Elastic Scattering Techniques

When soot particles in diffusion flames are irradiated by a pulsed laser sheet with a high power density, the particles emit elastic scattering and at the same time, increase their temperatures by absorbing part of the laser energy. Fig. 9 shows the temporal variations of temperature and radius of soot particles when a laser beam with a pulse duration of 20 ns heats the particles. The rise in particle temperature yields significant enhancement of thermal radiation and a shift of the peak wavelength of radiation to a shorter wavelength. At wavelengths shorter than 400 nm, the thermal radiation intensity from the incandescent soot particles at an elevated temperature of 4500 K is 2000 times higher than that from soot particles at a flame temperature of 2300 K. This permits the selective detection of the thermal radiation from incandescent soot particles which is nearly proportional to the soot volume fraction. This technique, called LII (Laser Induced Incandescence), is superior to the elastic scattering technique because it permits easy suppression of the elastic scattering from liquid droplets. The disadvantage of LII is that it requires high laser power to heat soot particles up to soot vaporization temperature, and that it is intrusive. The vaporized volume can be recovered in a time that the vaporized volume is filled by diffusion. These facts may limit the LII technique from obtaining images in quick succession.

On the other hand, the elastic scattering technique requires much less laser power because the emission intensity is around 100 times as high as that of LII technique. This allows its application to successive soot imaging at a short time interval. The intensity of elastic scattering from soot particles is known to be proportional to the sixth power of the diameter if the particle diameter to the incident light wavelength ratio is in the Rayleigh regime. This means that the scattering intensity is not necessarily proportional to the soot concentration if the diameter of soot particle is nonuniform. To make qualitative evaluation of the scattering technique, a comparison was made between the scattering and LII techniques.

The images of LII and scattering emission were both

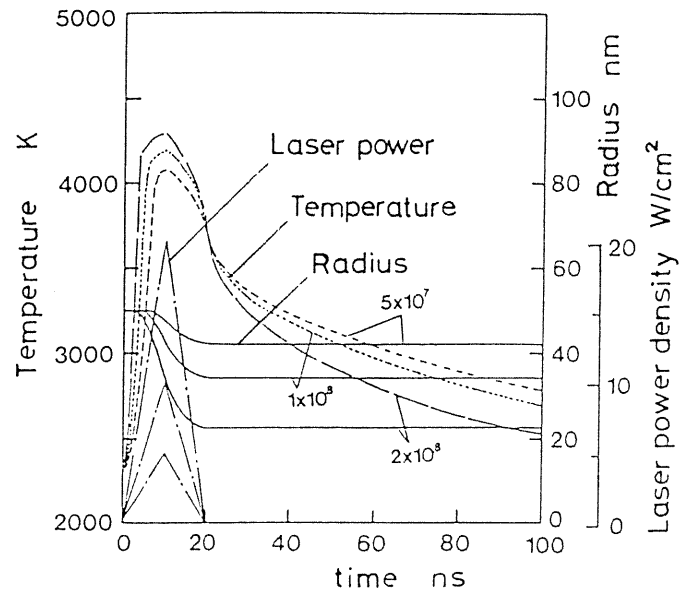


Fig. 9 Temporal variations of temperature and radius of soot when the power density of the incident laser light is changed

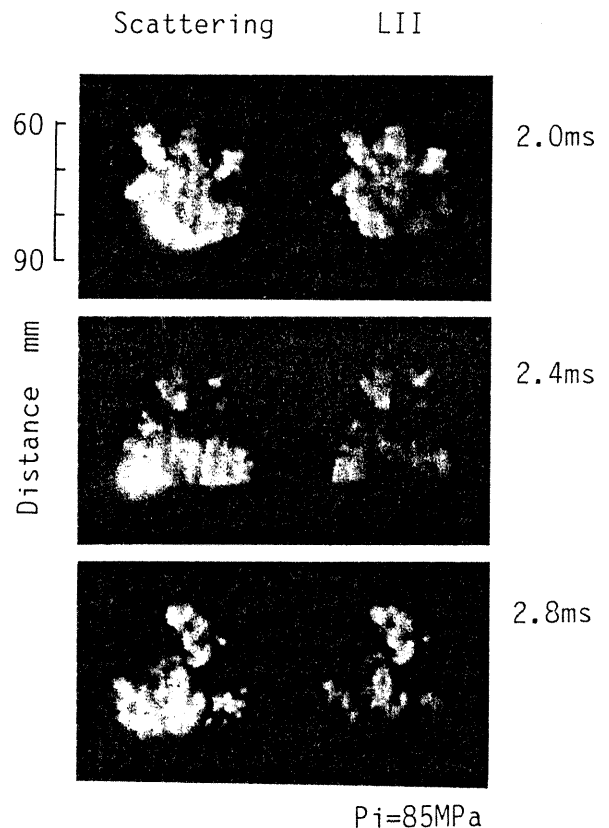


Fig. 10 Comparisons of 2-D soot images obtained by the elastic scattering technique and the LII technique

taken simultaneously using an ultra-violet half mirror and two sets of camera systems composed of a gated IIT and a CCD

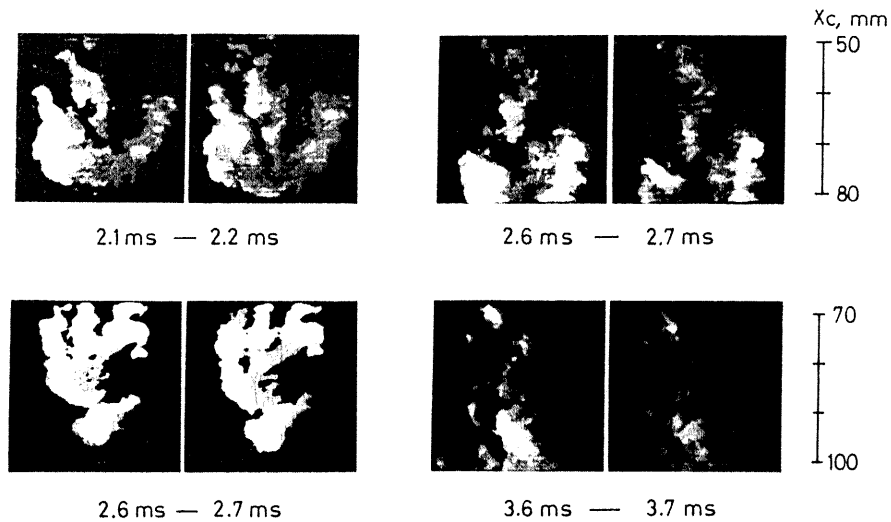


Fig. 11 Pairs of 2-D soot images taken at a time interval of 0.1 ms at various time after the start of injection

camera.[8] The method of LII is similar to that by Dec et al. [9], but differs in the use of the fundamental light of YAG laser at 1064 nm and the short wave pass filter with a cut-off wavelength of 40 nm. Laser output was 0.26 J per pulse, which resulted in a power level in the laser sheet about $4.3 \times 10^8 \text{ W/cm}^2$. In the elastic scattering imaging, a narrow band pass filter with center wavelength of 532 nm and FWHM of 4 nm was used to reduce the background continuous emission from soot particles. The effect of background luminosity was further suppressed by a short gated duration of 50 ns.

Fig. 10 shows typical results of simultaneous imaging. The region of strong scattering intensity coincides generally with the region of the strong LII signal. The general spatial consistence of the elastic scattering signal and LII signal implies that the regions of high elastic scattering can represent qualitatively the regions of high soot volume fraction. Consequently the elastic scattering technique was applied to obtaining two images in quick succession.

Elastic Scattering Technique[8]

To reduce the incident light attenuation by soot particles, a low sooting fuel composed of 20 % ethanol, 5 % octanol, and 75 % base fuel was used. The fuel was injected into a rapidly compressed air at a pressure of 2.7 MPa and a temperature of 900 K. The laser was double pulsed with a pulse interval of 0.1 ms, 10 ns individual pulse duration and 20 mJ individual pulse energy. The individual gate of the two cameras was synchronized to the individual laser pulse using a delay circuit.

taken simultaneously using an ultra-violet half mirror and two

Two-dimensional velocity distribution of soot clouds was estimated focusing on the spatial shift in scattering intensity pattern between an image pair. The spatial shift was determined by calculating the spatial cross correlation for all the pixels within a $4.5 \times 4.5 \text{ mm}$ square window. The velocity distribution measured with this technique is

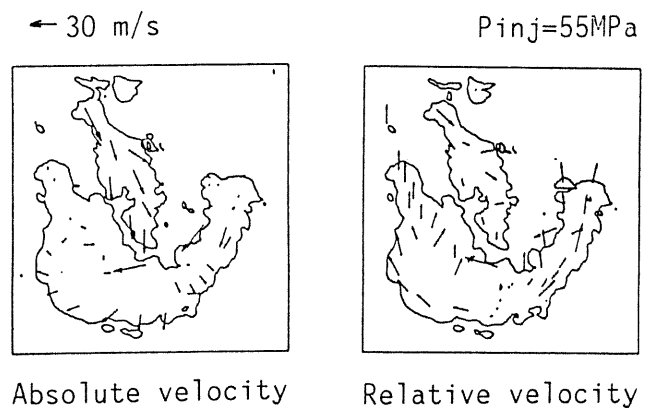


Fig. 12 Selected 2-D velocity vector distributions in a combusting spray[8]

qualitative at best because soot formation, oxidation, diffusion, and three dimensional convection will all affect the mean velocity.

Results and Discussions

Selected pairs of 2-D soot images taken at a time interval of 0.1 ms for an injection pressure of 55 MPa are shown in Fig. 11. t denotes time after the start of injection. The soot clouds of high scattering intensity can be sharply distinguished inside the flame, and their spatial scales are on the same order of magnitude as those of fuel vapor concentration distribution in evaporating sprays. It is worth noting that the periphery of the flame head present the highest intensity. Fig. 12 is a typical 2-D flow velocity distribution in the image taken at 2.1 ms. The velocity vectors relative to the flame tip velocity show the existence of a pair of twin vortices in the flame head which conveys soot from the central axis to the edge of the flame along the flame

boundary. This implies less air entrainment on the surface of the flame tip.

A comparison between 2-D soot images shown in Fig. 11 and 2-D fuel vapor concentration images shown in Fig. 8 indicates a feature that the equivalence ratio in the periphery of the spray where the highest soot concentration presents is far lower than stoichiometry. The reason for this is not clear, but a thorough inspection of the various image information obtained permits the following explanation: The soot being formed in rich mixtures along the spray axis travels downstream as increasing its concentration, and upon reaching the flame tip, it turns back being transported by a pair of twin vortices to the edge of the flame where the fuel concentration is low. The soot particles can generally oxidize very fast in a high temperature and oxygen rich environment, but in this situation, the temperature of soot particles on the surface of the flame appears to be cooled down by the surrounding air, resulting in slow soot oxidation. The dark appearance or low luminosity of the flame surface in the flame head which can be observed in direct photographs of the flame seems to support this hypothesis.

SUMMARY

Some of the techniques described in this paper are at the stage of practical application to the sprays in the engine cylinder with reasonable accuracy and reliability. The techniques that should be newly established in terms of diesel combustion studies are 2-D NO_x imaging and 2-D flame temperature pyrometry by means of OH radical fluorescence technique. These two techniques have been intensively tackled at several universities such as Pennsylvania State University[10] and Ruprecht-Karls-Universität Heidelberg.[11] These techniques will be hopefully available in the near future.

ACKNOWLEDGMENTS

The work discussed here is that of the students, Mr. Yeh, C-N., and Dr. Won, Y-H., and faculty; Mr. Kosaka, H. and Kobori, S., to whom I am greatly indebted. We are very grateful for the major support of this research which has come from a group research project, "Exploration of Combustion Mechanism", with a Grant-in-Aid for Scientific Research of Priority Area subsidized by the Ministry of Education, Science and Culture of Japan. The success of the work owed significantly to the use of the Nd-YAG laser provided by the above research group.

The image processing was carried out at the Advanced Intelligent Machine Complex at Tokyo Institute of Technology.

REFERENCES

1. Yeh, C-N., Kosaka, H., and Kamimoto, T., "Measurement of Drop Sizes in Unsteady Dense Sprays," Recent Advances in Spray Combustion, AIAA Progress Series, to be appeared in the near future.
2. Felton, P. G., Bracco, F. V., and Bardsley, M. E. A., "On the Quantitative Application of Exciplex Fluorescence to Engine Sprays," SAE Paper, 930870, 1993.
3. Reitz, R. D. and Diwaker, R., "Structure of High-Pressure Fuel Sprays," SAE Paper, 870598, 1987.
4. Gülder, Ö. L., Smallwood, G. J., and Snelling, D. R., "Diesel Spray Structure Investigation by Laser Diffraction and Sheet Illumination," SAE Paper, 920577, 1992.
5. Yeh, C-N., Kamimoto, T., Kobori, S., and Kosaka, H., "2-D Imaging of Fuel Vapor Concentration in a Diesel Spray via Exciplex-Based Fluorescence Technique," SAE Paper, 932652, 1993.
6. Melton, L. A. and Verdeck, J. F., "Vapor/Liquid Visualization for Fuel Sprays," Twentieth Symp. (Int.) on Comb., The Combustion Institute, pp.1283-1290, 1984.
7. Kosaka, H. and Kamimoto, T., "Quantitative Measurement of Fuel Vapor Concentration in an Unsteady Evaporating Spray via a 2-D Mie-Scattering Imaging Technique," SAE Paper, 932653, 1993.
8. Won, Y. H., Kamimoto, T., and Kosaka, H., "A Study on Soot Formation in Unsteady Spray Flames via 2-D Soot Imaging," SAE Paper, 9201143, 1992.
9. Dec, J. E., Zur Loye, A. O., and Siebers, D. L., "Soot Distribution in a D. I. Diesel Engine Using 2-D Laser-Induced Incandescence Imaging," SAE Paper, 910224, 1991.
10. Pinson, J. A., Mitchell, D. L., Santoro, R. J., and Litzinger, T. A., "Quantitative, Planar Soot Measurements in a D. I. Diesel Engine Using Laser-Induced Incandescence and Light Scattering," SAE Paper, 932650, 1993.
11. Arnold, A., Bräumer, A., Buschmann, A., Decker, M., Dinkelacker, F., Heitzmann, T., Orth, A., Schäfer, M., Sick, V., and Wolfrum, J., "2D-Diagnostics in Industrial Devices," Ber. Bunsenges. Phys. Chem. 97, pp.1650-1661, 1993.